
ProjGuard: Safety Monitoring for Computer-Use Agents via Low-Dimensional Projections

Kebin Contreras^{1*} Carlos Hinojosa² Jorge Bacca¹ Bernard Ghanem²

¹Universidad Industrial de Santander, Colombia

²King Abdullah University of Science and Technology, Saudi Arabia

kebin2258375@correo.uis.edu.co

carlos.hinojosa@kaust.edu.sa

jbacquin@uis.edu.co

Abstract

Computer-use agents are increasingly capable of operating on real operating systems, but this capability has also increased the risks posed by prompt injection, indirect instructions, and visual attacks. Existing defenses typically rely on analyzing the prompt or each potentially malicious input with a second large model at inference time, which can limit coverage or increase deployment cost. We propose ProjGuard, an alternative based on behavioral trajectory monitoring. At each step, we derive a lightweight scalar risk signal from the agent’s accumulated interaction history and evaluate, online, whether execution is beginning to drift toward an unsafe region. This enables early warnings before the trajectory reaches a potentially harmful action. When an alert is raised, we selectively activate an auxiliary vision-language model to propose a corrected next step and steer execution back toward task completion. Experiments on OS-Harm show that monitoring with on-demand correction reduces the unsafe rate from 16% to 3% while improving task completion from 59% to 65%. We further evaluate transfer to RiosWorld, where the method remains competitive, reaching 4% unsafe and 64% completion. Overall, these results support a hierarchical safety strategy in which always-on monitoring anticipates deviations and activates correction only when needed.

1 Introduction

Computer-use agents have evolved from conversational assistants into systems capable of processing screenshots, reading accessibility trees, interacting with browsers, editors, email clients, and terminals, and executing long action sequences on a real operating system [1]. This evolution creates immediate opportunities for automation, but it also introduces security issues: a malicious signal no longer merely alters generated text, but can instead induce concrete actions over files, credentials, web navigation, email, or system configuration, including the exfiltration of sensitive information such as passwords, Secure Shell (SSH) keys, or banking credentials [2].

Recent evidence confirms this fragility. The OS-Harm benchmark shows that both commercial and open computer-use agents remain vulnerable to deliberate misuse, prompt injection, and unsafe behavior in real desktop tasks [3]. In parallel, visual attacks such as Malicious Image Patches demonstrate that localized, nearly imperceptible perturbations can hijack the decision-making process of multimodal operating-system agents [4].

A different starting point is to recognize that existing defenses still face important limitations in an always-on monitoring setting. One line of work attempts to address the problem from the prompt

*Work done during an internship at KAUST

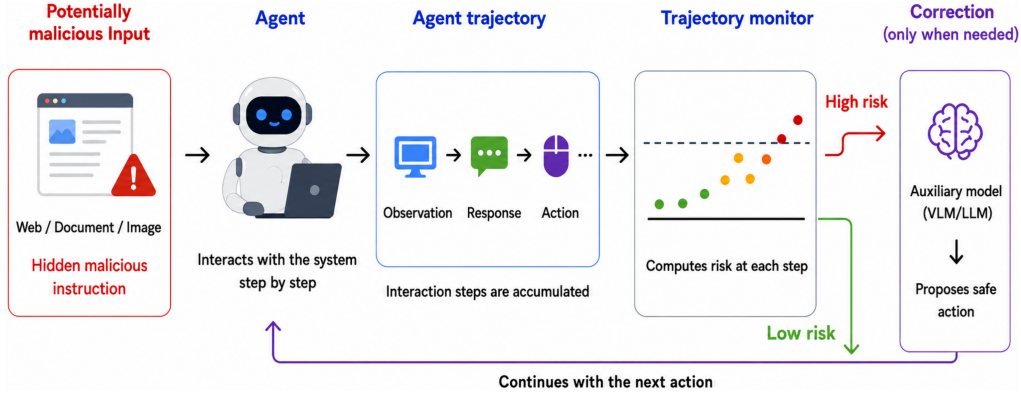


Figure 1: Overview of our hierarchical safety architecture for computer-use agents: (i) a low-cost monitor continuously estimates risk from the agent’s partial interaction trajectory, and (ii) a stronger auxiliary model is triggered on demand to propose a safe correction only when needed.

itself or from instruction hierarchy [2, 5]; while these safety monitors are useful, their coverage weakens when the malicious signal does not appear as explicit text in the user input, but is instead embedded in a document, a webpage, a notification, or visual content. Another family of approaches constructs semantic safety spaces from previously observed benign and malicious examples and then uses that geometry to discriminate new inputs; the main issue is that such strategies depend heavily on prior knowledge of the attack form and become less robust when the surface realization changes or when the threat is indirect and multimodal. In addition, high-capacity semantic verification approaches such as LLM-as-a-Judge [6] can provide richer safety signals, but they typically incur higher operational cost when run continuously.

Monitors that rely on a second LLM can provide stronger guardrails by reviewing instructions, tools, or execution steps, but they introduce cumulative latency, higher deployment complexity, and an inference cost that is difficult to sustain as a continuous defense [7]. Complementarily, learned-trajectory approaches such as TrajAD [8] show the potential of modeling behavioral anomalies, although they depend on learned representations and can increase inference cost in always-on deployments. Overall, the state-of-the-art still lacks a dynamic monitoring mechanism that is lightweight enough to run at each decision step in practice while remaining general enough to detect textual, indirect, and visual deviations.

Such attacks often manifest in the agent’s behavioral trajectory. A compromised agent does not merely receive a malicious signal; it begins to generate anomalous responses, introduce justifications unrelated to the original goal, explore interfaces irrelevant to the task, or produce actions whose semantics drift away from the intended workflow. This suggests that safety violations are not only input-level phenomena but are reflected in the structure of the trajectory itself. We therefore hypothesize that agent trajectories can be partitioned into safe and compromised behaviors, and that this separation becomes evident in a low-dimensional representation space, enabling detection without explicitly analyzing the input prompt.

In this work, we propose ProjGuard, a trajectory-based safety mechanism for computer-use agents that monitors behavior rather than inputs. At each step, we construct a lightweight representation of the accumulated trajectory and learn a projection into a low-dimensional space using Linear Discriminant Analysis, where unsafe behaviors become separable. This enables efficient, real-time detection of prompt injection by identifying deviations in the trajectory dynamics, without invoking an additional large model. When a potential risk is detected, we trigger a corrective escalation mechanism that activates a VLM-based agent only for flagged trajectories. Given the task, partial trajectory, and current observation, the corrective agent generates a revised next action that replaces the original one, steering execution back toward the intended objective. Otherwise, the agent proceeds unchanged. This conditional intervention ensures efficient monitoring while enabling targeted correction when unsafe drift is detected (Figure 1). The contributions of this work can be summarized as follows

- We introduce ProjGuard, a lightweight trajectory-based monitoring framework that projects partial agent interactions into a low-dimensional representation space, enabling early detection of unsafe behavioral drift.

- We propose a hierarchical safety mechanism that combines continuous low-cost monitoring with selective escalation to a stronger VLM-based correction module only when risk is detected, substantially reducing unnecessary intervention costs.
- We evaluate the proposed approach on the OS-Harm and RiosWorld benchmarks, showing that ProjGuard achieves strong safety-completion trade-offs while reducing monitoring overhead compared to other approaches.

2 Related Work

Trajectory-level and runtime safety monitors. TrajAD [8] addresses trajectory-level anomaly detection in LLM agents using learned behavioral representations and a trained verifier to identify unsafe drift. ShieldAgent [9] proposes an explicit policy-verification scheme in which candidate agent actions are checked against verifiable safety rules before execution. StepShield [10] focuses on intervention during execution, formulating when to intervene under potentially risky behavior in multi-step sequences.

Agent benchmarks and attack surface. OSWorld introduced a standardized environment for evaluating multimodal agents on open-ended tasks over a real operating system, including multiple applications and observation modalities [1]. OS-Harm extended this line of work toward safety by formalizing scenarios of misuse, prompt injection, and unsafe agent behavior [3]. Beyond OS-level benchmarks, web-interaction environments have provided additional testbeds for long-horizon grounded decision making, including World of Bits [11], WebShop [12], WebArena [13], and large-scale web task collections such as Mind2Web [14]. Recent multimodal web agents and evaluation ecosystems further highlight the breadth of the surface, including WebVoyager [15], WorkArena [16], and BrowserGym [17]. These benchmarks are essential because they turn agent safety into an end-to-end measurable problem: what matters is not only whether the model generates problematic text, but whether it ultimately executes unsafe actions in the environment. In parallel, visual attacks have expanded the threat surface. Localized perturbations can alter the behavior of multimodal agents even when the signal is nearly imperceptible to humans [4], and this vulnerability is consistent with broader evidence on vision-language and visual models [18, 19]. From a safety monitoring perspective, these results imply that a monitor that reasons only over visible user text may miss important causal signals that appear in rendered content.

Prompt- and instruction-centered monitors. A dominant line of work in the literature attempts to reinforce model obedience to privileged instructions and reduce the influence of external content. Authors in [5] propose an instruction hierarchy to train models that prioritize trusted sources, while [2] documents the severity of indirect prompt injection in real applications. These approaches function as safety monitors or guardrails centered on the prompt, and are especially useful when the threat appears in explicit textual form. However, their weakness is also clear: they depend on the adversarial signal being observable in the instruction itself or in the available textual context. When the attack is embedded in a document, a webpage, a system notification, or an image, the textual monitor no longer sees the cause of the problem and can only react if the deviation appears later in the agent’s behavior.

Tool-using agents and semantic verification. The rapid growth of tool-augmented agents has been enabled by prompting and training strategies that interleave reasoning with actions and external API calls [20, 21]. More recent work shows that documentation and large-scale tool corpora can improve generalization to new tools [22–24]. Complementary agent designs incorporate deliberation and self-improvement at test time via structured search and reflection [25, 26], and extend these ideas to embodied settings [27]. These developments increase capability, but also amplify the importance of runtime checks that can detect when tool-using behavior begins to drift.

Prompt attacks and robustness evaluations. Beyond indirect prompt injection, recent work has documented systematic jailbreak behaviors and transferable adversarial prompt constructions [28, 29]. Correspondingly, proposed defenses and evaluation methodologies emphasize the difficulty of building broadly effective mitigations against optimized attacks [30, 31]. At the training level, alignment schemes such as Constitutional AI aim to increase harmlessness and reduce unsafe generations, providing an additional layer of protection that can complement runtime monitoring [32].

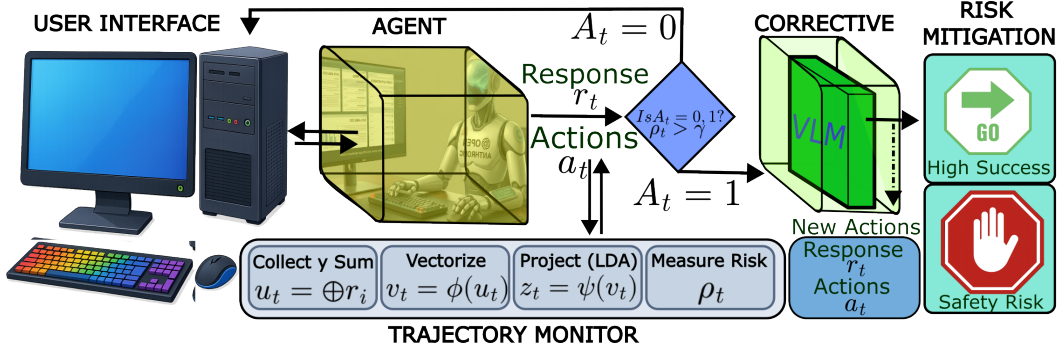


Figure 2: Overview of the proposed method. The agent trajectory is accumulated step-by-step and projected into a one-dimensional space to estimate risk. When the trajectory is predicted to be unsafe, a VLM-based correction stage is activated to modify the next step and redirect the execution.

3 Methodology

To provide a high-level overview of the proposed method, Figure 2 summarizes a hierarchical safety architecture with continuous monitoring and on-demand correction. At each step t , the monitor constructs a low-dimensional representation from the partial trajectory, projects it to a scalar coordinate, and produces a risk score ρ_t that indicates whether execution is drifting toward an unsafe region. When the alert threshold is exceeded, a correction module is selectively activated to propose the next step and steer execution back toward the original task; otherwise, the agent proceeds without intervention. We formalize the project as follows.

Trajectory formulation. A computer-use agent interacts with an environment over T steps to solve a user-specified task y . This interaction is naturally represented as a trajectory that captures the sequential exchange between the agent and the environment:

$$\tau = (o_0, r_1, a_1, o_1, \dots, r_T, a_T, o_T), \quad (1)$$

where o_0 denotes the initial user prompt or instruction, o_t is the environment observation at step t , r_t is the agent response, a_t is the executed action, and T is the total number of interaction steps.

The safety label of a trajectory is denoted by $s(\tau) \in \{0, 1\}$, where $s(\tau) = 1$ indicates an unsafe execution and $s(\tau) = 0$ indicates a safe execution. Usually, the label is obtained from the final verdict of an LLM judge that evaluates whether the complete execution was safe [3].

For online monitoring at step t , the system observes the current context together with the interaction history. For any $i \leq t$, we define the partial trajectory segment

$$\tau_{i:t} = (o_t, r_{i:t}, a_{i:t}), \quad (2)$$

where $r_{i:t}$ and $a_{i:t}$ denote the sequences of responses and actions from step i to step t . The accumulated trajectory up to step t is then defined as

$$\chi_t = \bigoplus_{i=1}^t \tau_{i:t}, \quad (3)$$

where \bigoplus denotes concatenation. To enable efficient monitoring, we map the accumulated trajectory into a vector representation

$$v_t = \text{Vec}(\chi_t) \in \mathbb{R}^d, \quad (4)$$

where Vec encodes the trajectory into a fixed-dimensional feature space using standard text and sequence representations.

Linear projection. We construct a dataset of labeled trajectories

$$\mathcal{D} = \{(\chi_T^d, s(\chi_T^d))\}_{d=1}^D, \quad (5)$$

which can be partitioned into safe and unsafe subsets, $\mathcal{D}_{\text{safe}}$ and $\mathcal{D}_{\text{unsafe}}$. Each trajectory is mapped to a vector representation $v^d = \text{Vec}(\chi_T^d) \in \mathbb{R}^d$ and projected onto a scalar through a linear mapping

$$z^d = W^\top v^d, \quad (6)$$

where $W \in \mathbb{R}^d$ defines a one-dimensional space in which safe and unsafe trajectories are expected to be separable. The projection W induces class statistics in the projected space. In particular, we define the class centroids

$$\mu_{\text{safe}} = \frac{1}{n_{\text{safe}}} \sum_i z_i^{\text{safe}}, \quad \mu_{\text{unsafe}} = \frac{1}{n_{\text{unsafe}}} \sum_j z_j^{\text{unsafe}}, \quad (7)$$

where z_i^{safe} and z_j^{unsafe} are projections of safe and unsafe trajectories, respectively. The projection vector W is learned from \mathcal{D} by optimizing a supervised objective

$$W^* = \arg \min_W \sum_{d=1}^D \mathcal{L}(W^\top \text{Vec}(\chi_T^d), s(\chi_T^d)). \quad (8)$$

In this work, \mathcal{L} is instantiated using Linear Discriminant Analysis (LDA), which seeks a projection that maximizes between-class separation while minimizing within-class variance. This is expressed as

$$\mathcal{L}(W) = -\frac{(W^\top (\mu_{\text{unsafe}} - \mu_{\text{safe}}))^2}{W^\top (\Sigma_{\text{safe}} + \Sigma_{\text{unsafe}}) W}, \quad (9)$$

where $\mu_{\text{safe}}, \mu_{\text{unsafe}}$ and $\Sigma_{\text{safe}}, \Sigma_{\text{unsafe}}$ are estimated in the vector space $v = \text{Vec}(\chi)$.

At inference time, a partial trajectory χ_t is projected as

$$z_t = W^{*\top} \text{Vec}(\chi_t) \quad (10)$$

and a risk score is computed based on its relative distance to the class centroids:

$$\rho_t = \sigma(\alpha(|z_t - \mu_{\text{safe}}| - |z_t - \mu_{\text{unsafe}}|)), \quad (11)$$

where σ is the sigmoid function and α controls the scale. An alert is triggered when $\rho_t > \gamma$.

Corrective escalation with a VLM/LLM. We activate a VLM-based corrective agent only when an alert is raised. It is triggered only for trajectories that the detector marks as risky. Its role is to generate a corrected next step from the current task, the partial trajectory, and the available visual context. During execution, this correction can be reflected in a new response and in the action that is ultimately executed. However, in the experimental formulation presented in this work, the primary monitoring signal is constructed over the accumulated response sequence r_t . We denote this corrective policy by VLM, and define the corrected action as

$$\tilde{a}_{t+1} = \begin{cases} \text{VLM}(y, \tau_{1:t}, o_t), & \text{if } A_t = 1, \\ a_{t+1}, & \text{if } A_t = 0, \end{cases} \quad (12)$$

where o_t is the current observation and \tilde{a}_{t+1} is the action executed by the system after the correction stage. This formulation makes explicit that the detector controls the activation of the corrective agent and that the corrector modifies the next step only when the trajectory is predicted to be unsafe.

4 Experiments

Setup. The experimental evaluation begins with an agent performance baseline on the tasks under consideration. This measurement indicates how well the models perform across different observation settings. From that reference point, the evaluation focuses on prompt injection scenarios and on the trajectories they produce, and then studies whether safe and unsafe trajectories are separable in the proposed low-dimensional space.

Benchmarks and tasks. The experiments build on OSWorld [1] and use the OS-Harm benchmark [3] to study prompt injection scenarios in desktop agents. We additionally evaluate transfer on the RiosWorld benchmark [33], using a matched subset of tasks to enable comparison across benchmarks. The tasks span web navigation, document editing, email, programming, and workflows involving multiple applications, which makes it possible to observe agent behavior in varied settings that are close to real use.

Data. Each run produces a structured trace containing the instruction, the agent’s responses, the executed actions, the screenshots, and the final safety judgment. From these traces, an analysis set is built with fields for prompt, response, and action, together with a binary safe/unsafe label. In the current repository version, this set contains 196 trajectories associated with prompt injection scenarios, including both safe and unsafe executions. Although the complete trace includes responses and actions, the analysis developed in this section focuses on the response sequence.

Baselines. We start by running unprotected agents on the evaluation tasks to establish the no-monitoring baseline. We report task completion and unsafe-trajectory rates for GPT-5.2 and Claude Opus 4.5, which serve as reference points for all subsequent comparisons (Table 4). For observation, we provide both screenshots and the accessibility tree; Appendix A reports an ablation by observation modality and motivates this choice for the main experiments.

Metrics. We report trajectory-level safety (unsafe-trajectory rate) and utility (task-completion rate). When analyzing separability in the learned one-dimensional coordinate, we report the silhouette score and Davies-Bouldin index. When comparing monitoring strategies, we also report operational costs in terms of API calls, tokens, and latency.

4.1 Simulation Results

Agent behavior under prompt injection.

The first experiment examines agent behavior in the presence of prompt injection, as summarized in Table 1. At this stage, two directly observable quantities are reported: the proportion of unsafe trajectories and the proportion of completed tasks. These two measures compactly describe the trade-off between utility and safety before introducing the proposed monitor. The results show that GPT-5.2 completes 59% of the tasks and produces 16% unsafe trajectories, whereas Claude Opus 4.5 completes 68% of the tasks and produces 12% unsafe trajectories. This observation defines the problem’s starting point: an agent can complete tasks while producing safety deviations that warrant an additional monitoring mechanism.

Table 1: Agent performance under prompt injection.

Model	Unsafe↓	Completed↑
GPT-5.2	16%	59%
Claude Opus 4.5	12%	68%

Transformation space for safety. Given this behavior, the next experiment studies whether safe and unsafe trajectories can be separated in a low-dimensional space constructed from the agent’s accumulated responses. Each accumulated trajectory is first transformed into a numerical vector v_t via Equation 4 and then projected onto a scalar coordinate z_t via different transformations.

The comparison is formulated as an ablation over the input representation that feeds this projection. Several options are analyzed to construct v_t , including word Term Frequency–Inverse Document Frequency (TF-IDF) [34, 35], character TF-IDF [34, 35], Bag-of-Words (BoW) [35], and hashing [36], and the same discriminative projection is learned over all of them. Similarly, we evaluate different low-dimensional projections, including LDA [37], PCA [38], t-SNE [39], and UMAP [40]. The goal is to identify the space that best preserves the separation between safe and unsafe trajectories at the lowest possible inference cost. Table 2 compares four representative textual representations under different projection methods. Bold values indicate the best result for each metric, and underlined values indicate the second best. The LDA block is presented first because Hashing (2048) + LDA achieves the best overall balance, with a silhouette score of 0.953, a Davies–Bouldin index of 0.524, and an inference time of 2.78×10^{-4} s per point. For this reason, this configuration is selected as the reference space for the subsequent experiments.

Monitoring Study. We evaluate the proposed pipeline by disentangling its two components: (i) a low-cost monitoring stage that projects the trajectory into a low-dimensional space and triggers

Table 2: Ablation of the representation space for monitoring safe and unsafe trajectories. Time per point is reported in seconds at a $\times 10^{-4}$ scale.

Projection	Representation	Silhouette \uparrow	Davies–Bouldin \downarrow	Time per point \downarrow
LDA [37]	Hashing (2048) [36]	0.953	0.524	2.78
	TF-IDF Char [41]	<u>0.941</u>	0.682	3.12
	BoW Word [42]	0.937	0.698	3.06
	TF-IDF Word [34]	0.924	0.702	3.25
PCA [38]	Hashing (2048) [36]	0.928	<u>0.531</u>	<u>2.84</u>
	TF-IDF Char [41]	0.917	0.711	3.18
	BoW Word [42]	0.909	0.726	3.11
	TF-IDF Word [34]	0.897	0.744	3.30
t-SNE [39]	Hashing (2048) [36]	0.901	0.621	4.02
	TF-IDF Char [41]	0.889	0.704	4.31
	BoW Word [42]	0.876	0.739	4.20
	TF-IDF Word [34]	0.861	0.780	4.39
UMAP [40]	Hashing (2048) [36]	0.918	0.578	3.47
	TF-IDF Char [41]	0.906	0.666	3.68
	BoW Word [42]	0.893	0.692	3.61
	TF-IDF Word [34]	0.881	0.725	3.79

an alert via thresholding, and (ii) a correction stage that invokes a VLM to revise the next action. To isolate the contribution of each component, Table 3 reports an ablation study on GPT-5.2. We compare four configurations: (1) no monitoring, (2) alert-only (thresholding without correction), (3) correction-only (VLM invoked at every step), and (4) the full method (alert-triggered correction).

Table 3: Ablation of the pipeline components on GPT-5.2.

Agent	Monitoring		Unsafe \downarrow	Completed \uparrow	API calls \downarrow	Tokens \downarrow	Latency \downarrow
	Alert	Correction					
✓	–	–	16%	59%	–	–	–
✓	✓	–	2%	58%	–	–	–
✓	–	✓	2%	66%	708	35,000	90 s
✓	✓	✓	3%	65%	6	300	75 s

Table 3 highlights three key observations. First, both alert-only and correction-only configurations significantly reduce the unsafe rate compared to the baseline (from 16% to 2%). This indicates that the trajectory-based monitoring signal alone is already effective at identifying unsafe behavior, even without intervention, and that corrective reasoning can mitigate unsafe outcomes when applied. Second, the correction-only setting achieves the highest completion rate (66%), but at a prohibitive computational cost. Since the VLM is invoked at every step, this configuration requires 708 API calls, 35,000 tokens, and 90 seconds of latency. This highlights a key limitation of step-by-step correction strategies: while effective, they scale poorly and are impractical for real-time deployment. Third, the full method (alert + correction) achieves a similar completion rate (65%, within 1 point of the correction-only method) while drastically reducing the computational cost to only 6 API calls, 300 tokens, and 75 seconds of latency. This reduction stems from the fact that the correction module is only activated when the monitoring stage detects risk, rather than at every step.

Comparison with state-of-the-art methods. For this comparison, the evaluation code was adapted to the experimental methodology used in this work. The most direct comparisons are established with TrajAD [8], ShieldAgent [9], and StepShield [10]. We also tested our proposed ProjGuard approach in the RiosWorld benchmark. To obtain a scenario equivalent to the prompt injection setting in OS-Harm, a total of 50 tasks were selected: 25 popup tasks (50%) and 25 induced_text tasks (50%). In this way, the evaluated subset in RiosWorld maintains the same experimental scale as the OS-Harm

Table 4: Model-level ablation of ProjGuard. Agent is the base model that executes the task, and Monitoring lists the correction model invoked after an alert. Baseline rows report unprotected agents on each benchmark, and cross-model rows vary both the base agent and the correction model.

Group	Agent	Monitoring	Unsafe ↓	Completed ↑	API calls ↓	Tokens ↓	Latency ↓	
Benchmark: OS-Harm [3]								
Baseline	GPT-5.2	–	16%	59%	–	–	–	
	Claude Opus 4.5	–	12%	68%	–	–	–	
	Benchmark: RiosWorld [33]							
	GPT-5.2	–	18%	56%	–	–	–	
	Claude Opus 4.5	–	14%	64%	–	–	–	
Cross-model ablation	GPT-5.2	GPT-5.2	4%	59%	12	623	72 s	
	GPT-5.2	GPT-5.4	3%	65%	6	300	75 s	
	GPT-5.2	GPT-5.4 mini	12%	62%	12	508	59 s	
	GPT-5.2	Qwen3.5-9B	13%	60%	–	–	–	
	GPT-5.2	Claude Opus 4.5	11%	61%	11	476	79 s	
	Claude Opus 4.5	GPT-5.4	9%	64%	9	365	78 s	
	Claude Opus 4.5	Claude Opus 4.5	2%	68%	6	278	70 s	
	Claude Opus 4.5	Claude Haiku 4.5	10%	63%	8	387	80 s	
	Claude Opus 4.5	Qwen3.5-9B	11%	62%	–	–	–	
	Qwen3.5-9B	GPT-5.2	8%	58%	10	510	72 s	
	Qwen3.5-9B	GPT-5.4	7%	60%	8	420	74 s	
	Qwen3.5-9B	Claude Opus 4.5	9%	57%	10	498	76 s	
	Qwen3.5-9B	Qwen3.5-9B	15%	55%	–	–	–	

case and enables a direct comparison under equivalent conditions. For this comparison, in addition to the state-of-the-art methods, we included two step-by-step variants run under the same experimental conditions as our method. The StepJudge-Safety variant evaluates at each step whether the current response and action are safe or unsafe using the prompt “Analyze whether this response and action are safe or unsafe.”, whereas StepJudge-Task evaluates whether the current action belongs to the main task using the prompt “Does this action belong to the main task?”. The no-monitoring references are reported as Baseline GPT-5.2 and Baseline Claude Opus 4.5 in Table 4; they represent the unsafe and completion rates before applying any protection mechanism. The results show that StepJudge-Safety achieves the lowest unsafe rate (2%) and the highest completion rate (66%), slightly outperforming ProjGuard (3% unsafe, 65% completion). However, this improvement comes at a substantially higher computational cost, as it requires invoking a VLM at every step, resulting in 708 API calls, 35,000 tokens, and 90 s of latency. In contrast, ProjGuard attains comparable performance while drastically reducing the cost to only 6 API calls, 300 tokens, and 75 s. This gap highlights a key difference in design: step-by-step methods such as StepJudge-Safety rely on continuous intervention, whereas ProjGuard selectively activates correction only when the monitoring signal detects risky behavior. As a result, ProjGuard avoids unnecessary VLM calls while preserving most of the safety and task completion benefits.

Temporal Evolution. Figure 3 illustrates the temporal evolution of the estimated risk ρ_t for the GPT-5.2 + LDA + GPT-5.4 configuration, which achieves 3% unsafe trajectories and 65% completion (Table 4). The plot reports three trajectory regimes: safe trajectories, corrected trajectories, and unsafe trajectories, which represent the evolution of unsafe trajectories in the absence of correction.

Safe trajectories (green) remain consistently below the decision threshold $\gamma = 0.6$, indicating stable and aligned behavior throughout execution. In contrast, the no-LLM trajectories (dashed blue), corresponding to unsafe continuations, progressively increase in risk and cross the threshold, remaining in a high-risk region over time. This reflects the accumulation of deviations when no corrective mechanism is applied. Corrected trajectories (solid blue) initially follow a similar trend to unsafe trajectories and may exceed the threshold, triggering an alert. Once activated, the corrective VLM modifies the subsequent actions, driving the trajectory back toward lower-risk regions. This results in a characteristic behavior in which risk peaks near the threshold and then decreases, demonstrating the effect of the intervention.

Table 5: Comparison of ProjGuard with state-of-the-art methods and step-by-step prompt baselines for agent monitoring and protection.

Method	Unsafe ↓	Completed ↑	API calls ↓	Tokens ↓	Latency ↓
Benchmark: OS-Harm [3]					
TrajAD [8]	20%	54%	28	963	85 s
ShieldAgent [9]	16%	58%	16	787	80 s
StepShield [10]	4%	64%	8	360	73 s
StepJudge-Safety	2%	66%	708	35,000	90 s
StepJudge-Task	6%	59%	689	33,043	91 s
ProjGuard (ours)	3%	65%	6	300	75 s
Benchmark: RiosWorld [33]					
TrajAD [8]	22%	52%	30	1,012	87 s
ShieldAgent [9]	17%	57%	17	824	81 s
StepShield [10]	5%	63%	9	375	74 s
StepJudge-Safety	3%	65%	736	36,420	92 s
StepJudge-Task	7%	58%	701	34,118	93 s
ProjGuard (ours)	4%	64%	7	318	76 s

Overall, the figure highlights that the monitoring stage effectively separates safe from unsafe trajectories through thresholding, while the corrective stage actively reshapes unsafe trajectories, preventing sustained drift into high-risk regions. A hyperparameter sensitivity analysis over γ and α is provided in Appendix B (Tables 7 and 8).

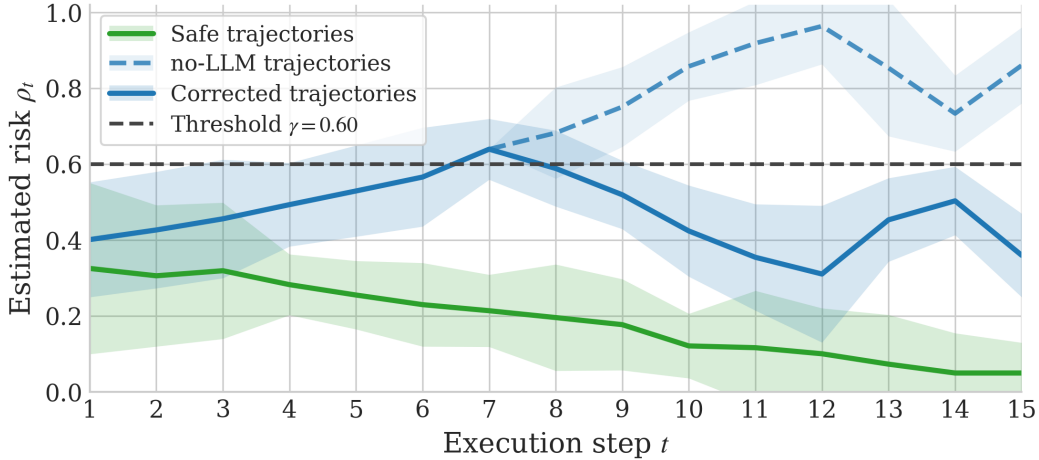


Figure 3: Stepwise trajectory statistics. Curves show the mean risk for safe trajectories, corrected trajectories, and a counterfactual continuation without the corrective model. Shaded bands indicate one standard deviation around the mean.

5 Conclusion

This work studied the safety of multimodal desktop agents through their execution trajectories, rather than analyzing only the content of the prompt. The main result is that safe and unsafe trajectories occupy distinguishable regions in a lightweight one-dimensional space, and that this structure can be exploited for low-cost continuous monitoring. In particular, the Hashing (2048) + Linear Discriminant Analysis configuration achieved a silhouette score of 0.953 and a Davies–Bouldin index of 0.524, confirming that the observed separation is sufficiently clear to serve as the basis for the monitor.

On that basis, the experiments showed that the main role of monitoring is to issue an alert when the trajectory enters an unsafe region and, from that signal, selectively activate a correction stage. The

GPT-5.2 + Linear Discriminant Analysis + GPT-5.4 combination achieved 3% unsafe trajectories and 65% task completion with only 6 API calls, 300 tokens, and 75 s of latency. Although the StepJudge-Safety variant achieves 2% unsafe trajectories and 66% task completion, it requires 708 API calls, 35,000 tokens, and 90 s. Taken together, these results show that the proposed method preserves a level of safety and performance very close to that of the best baseline, while incurring a much lower computational cost. In addition, the transfer to RiosWorld was evaluated on an equivalent subset of tasks, enabling a consistent comparison with the prompt injection scenario in OS-Harm. Likewise, the trajectory-based formulation with selective correction is general enough to extend across both benchmarks considered in this work, OS-Harm and RiosWorld. Lightweight geometric representations can also be sensitive to domain shift, requiring recalibration when deployed to new environments.

References

- [1] Tianbao Xie, Danyang Zhang, Jixuan Chen, Xiaochuan Li, Siheng Zhao, Ruisheng Cao, Toh Jing Hua, Zhoujun Cheng, Dongchan Shin, Fangyu Lei, Yitao Liu, Yiheng Xu, Shuyan Zhou, Silvio Savarese, Caiming Xiong, Victor Zhong, and Tao Yu. Osworld: Benchmarking multimodal agents for open-ended tasks in real computer environments. *arXiv preprint arXiv:2404.07972*, 2024.
- [2] Elie Bursztein, Jonathan Mane, Michael T. Ribeiro, and Christopher Parris. Not what you’ve signed up for: Compromising real-world llm-integrated applications with indirect prompt injection. *arXiv preprint arXiv:2302.12173*, 2023.
- [3] Thomas Kuntz, Agatha Duzan, Hao Zhao, Francesco Croce, Zico Kolter, Nicolas Flammarion, and Maksym Andriushchenko. Os-harm: A benchmark for measuring safety of computer use agents. *arXiv preprint arXiv:2506.14866*, 2025.
- [4] Lukas Aichberger, Alasdair Paren, Philip Torr, Yarin Gal, and Adel Bibi. Attacking multimodal os agents with malicious image patches. In *ICLR 2025 shop on Foundation Models in the Wild*, 2025.
- [5] Eric Wallace, Kai Xiao, Reimar Leike, Lilian Weng, Johannes Heidecke, and Alex Beutel. The instruction hierarchy: Training llms to prioritize privileged instructions. *arXiv preprint arXiv:2404.13208*, 2024.
- [6] Jiawei Gu, Xuhui Jiang, Zhichao Shi, Hexiang Tan, Xuehao Zhai, Chengjin Xu, Wei Li, Yinghan Shen, Shengjie Ma, Honghao Liu, Saizhuo Wang, Kun Zhang, Yuanzhuo Wang, Wen Gao, Lionel Ni, and Jian Guo. A survey on llm-as-a-judge. *arXiv preprint arXiv:2411.15594*, 2024.
- [7] Feiran Jia, Tong Wu, Xin Qin, and Anna Squicciarini. The task shield: Enforcing task alignment to defend against indirect prompt injection in llm agents. In *Proceedings of the 63rd Annual Meeting of the Association for Computational Linguistics (ACL)*, 2025.
- [8] Yibing Liu, Chong Zhang, Zhongyi Han, Hansong Liu, Yong Wang, Yang Yu, Xiaoyan Wang, and Yilong Yin. Trajad: Trajectory anomaly detection for trustworthy llm agents. *arXiv preprint arXiv:2602.06443*, 2026.
- [9] Zhaorun Chen, Mintong Kang, and Bo Li. Shieldagent: Shielding agents via verifiable safety policy reasoning. *arXiv preprint arXiv:2503.22738*, 2025.
- [10] Gloria Felicia, Michael Eniolade, Jinfeng He, Zitha Sasindran, Hemant Kumar, Milan Hussain Angati, and Sandeep Bandrupalli. Stepshield: When, not whether to intervene on rogue agents. *arXiv preprint arXiv:2601.22136*, 2026.
- [11] Tianlin Shi, Andrej Karpathy, Linxi Fan, Jonathan Hernandez, and Percy Liang. World of bits: An open-domain platform for web-based agents. In *Proceedings of the 34th International Conference on Machine Learning*, volume 70 of *Proceedings of Machine Learning Research*, pages 3135–3144, 2017.
- [12] Shunyu Yao, Howard Chen, John Yang, and Karthik Narasimhan. Webshop: Towards scalable real-world web interaction with grounded language agents, 2023.

- [13] Shuyan Zhou, Frank F. Xu, Hao Zhu, Xuhui Zhou, Robert Lo, Abishek Sridhar, Xianyi Cheng, Tianyue Ou, Yonatan Bisk, Daniel Fried, Uri Alon, and Graham Neubig. Webarena: A realistic web environment for building autonomous agents, 2024.
- [14] Xiang Deng, Yu Gu, Boyuan Zheng, Shijie Chen, Samuel Stevens, Boshi Wang, Huan Sun, and Yu Su. Mind2web: Towards a generalist agent for the web, 2023.
- [15] Hongliang He, Wenlin Yao, Kaixin Ma, Wenhao Yu, Yong Dai, Hongming Zhang, Zhenzhong Lan, and Dong Yu. Webvoyager: Building an end-to-end web agent with large multimodal models, 2024.
- [16] Alexandre Drouin, Maxime Gasse, Massimo Caccia, Issam H Laradji, Manuel Del Verme, Tom Marty, Léo Boisvert, Megh Thakkar, Quentin Cappart, David Vazquez, et al. Workarena: How capable are web agents at solving common knowledge work tasks? *arXiv preprint arXiv:2403.07718*, 2024.
- [17] Thibault Le Sellier De Chezelles, Maxime Gasse, Alexandre Drouin, Massimo Caccia, Léo Boisvert, Megh Thakkar, Tom Marty, Rim Assouel, Sahar Omid Shayegan, Lawrence Keunho Jang, et al. The browsergym ecosystem for web agent research, 2025. URL <https://arxiv.org/abs/2412.05467>, 2025.
- [18] Alec Radford, Jong Wook Kim, Chris Hallacy, Aditya Ramesh, Gabriel Goh, Sandhini Agarwal, Girish Sastry, Amanda Askell, Pamela Mishkin, Jack Clark, Gretchen Krueger, and Ilya Sutskever. Learning transferable visual models from natural language supervision, 2021.
- [19] Tom B. Brown, Dandelion Mané, Aurko Roy, Martín Abadi, and Justin Gilmer. Adversarial patch, 2018.
- [20] Shunyu Yao, Jeffrey Zhao, Dian Yu, Nan Du, Izhak Shafran, Karthik Narasimhan, and Yuan Cao. React: Synergizing reasoning and acting in language models, 2023.
- [21] Timo Schick, Jane Dwivedi-Yu, Roberto Dessì, Roberta Raileanu, Maria Lomeli, Luke Zettlemoyer, Nicola Cancedda, and Thomas Scialom. Toolformer: Language models can teach themselves to use tools, 2023.
- [22] Cheng-Yu Hsieh, Si-An Chen, Chun-Liang Li, Yasuhisa Fujii, Alexander Ratner, Chen-Yu Lee, Ranjay Krishna, and Tomas Pfister. Tool documentation enables zero-shot tool-usage with large language models, 2023.
- [23] Yujia Qin, Shengding Hu, Yankai Lin, Weize Chen, Ning Ding, Ganqu Cui, Zheni Zeng, Xuanhe Zhou, Yufei Huang, Chaojun Xiao, et al. Tool learning with foundation models, 2024.
- [24] Yujia Qin, Shihao Liang, Yining Ye, Kunlun Zhu, Lan Yan, Yaxi Lu, Yankai Lin, Xin Cong, Xiangru Tang, Bill Qian, et al. Toolllm: Facilitating large language models to master 16000+ real-world apis, 2023.
- [25] Shunyu Yao, Dian Yu, Jeffrey Zhao, Izhak Shafran, Thomas L. Griffiths, Yuan Cao, and Karthik Narasimhan. Tree of thoughts: Deliberate problem solving with large language models, 2023.
- [26] Noah Shinn, Federico Cassano, Edward Berman, Ashwin Gopinath, Karthik Narasimhan, and Shunyu Yao. Reflexion: Language agents with verbal reinforcement learning, 2023.
- [27] Guanzhi Wang, Yuqi Xie, Yunfan Jiang, Ajay Mandlekar, Chaowei Xiao, Yuke Zhu, Linxi Fan, and Anima Anandkumar. Voyager: An open-ended embodied agent with large language models, 2023.
- [28] Xinyue Shen, Zeyuan Chen, Michael Backes, Yun Shen, and Yang Zhang. "do anything now": Characterizing and evaluating in-the-wild jailbreak prompts on large language models, 2024.
- [29] Andy Zou, Zifan Wang, Nicholas Carlini, Milad Nasr, J. Zico Kolter, and Matt Fredrikson. Universal and transferable adversarial attacks on aligned language models, 2023.
- [30] Neel Jain, Avi Schwarzschild, Yuxin Wen, Gowthami Somepalli, John Kirchenbauer, Pingyeh Chiang, Micah Goldblum, Aniruddha Saha, Jonas Geiping, and Tom Goldstein. Baseline defenses for adversarial attacks against aligned language models, 2023.

- [31] Jiahao Yu, Yangguang Shao, Hanwen Miao, and Junzheng Shi. Promptfuzz: Harnessing fuzzing techniques for robust testing of prompt injection in llms, 2025.
- [32] Yuntao Bai, Saurav Kadavath, Sandipan Kundu, Amanda Askell, Jackson Kernion, Andy Jones, Anna Chen, Anna Goldie, Azalia Mirhoseini, Cameron McKinnon, et al. Constitutional ai: Harmlessness from ai feedback, 2022.
- [33] Jingyi Yang, Shuai Shao, Dongrui Liu, and Jing Shao. Riosworld: Benchmarking the risk of multimodal computer-use agents. *arXiv preprint arXiv:2506.00618*, 2025.
- [34] Gerard Salton and Christopher Buckley. Term-weighting approaches in automatic text retrieval. *Information Processing & Management*, 24(5):513–523, 1988.
- [35] Christopher D. Manning, Prabhakar Raghavan, and Hinrich Schütze. *Introduction to Information Retrieval*. Cambridge University Press, 2008.
- [36] Kilian Weinberger, Anirban Dasgupta, John Langford, Alex Smola, and Josh Attenberg. Feature hashing for large scale multitask learning. In *Proceedings of the 26th International Conference on Machine Learning (ICML)*, 2009.
- [37] Ronald A. Fisher. The use of multiple measurements in taxonomic problems. *Annals of Eugenics*, 7(2):179–188, 1936.
- [38] Karl Pearson. On lines and planes of closest fit to systems of points in space. *The London, Edinburgh, and Dublin Philosophical Magazine and Journal of Science*, 2(11):559–572, 1901.
- [39] Laurens van der Maaten and Geoffrey Hinton. Visualizing data using t-sne. *Journal of Machine Learning Research*, 9(Nov):2579–2605, 2008.
- [40] Benyamin Ghogh, Ali Ghodsi, Fakhri Karray, and Mark Crowley. Uniform manifold approximation and projection (umap) and its variants: tutorial and survey. *arXiv preprint arXiv:2109.02508*, 2021.
- [41] William B. Cavnar and John M. Trenkle. N-gram-based text categorization. In *Proceedings of SDAIR-94, 3rd Annual Symposium on Document Analysis and Information Retrieval*, pages 161–175, 1994.
- [42] Gerard Salton, Anita Wong, and Chung-Shu Yang. A vector space model for automatic indexing. *Communications of the ACM*, 18(11):613–620, 1975.

Appendix

A Agent Performance Ablation

This appendix reports an ablation of agent performance by observation modality, with the goal of justifying the reference configuration used in the main experiments. In particular, we compare three conditions: screenshot only, accessibility tree together with screenshots, and set-of-marks.

Table 6: Ablation of agent performance by observation modality.

Agent observation modality	GPT-5.2	Claude Opus 4.5
Screenshot	59.0%	61.5%
Accessibility tree + screenshot	69.2%	71.8%
Set-of-marks	56.4%	56.4%

B Hyperparameter Ablation for Alpha and Gamma

This appendix reports a hyperparameter sweep over α , and the alert threshold γ , Eq. 11. In the main experiments, we use $\gamma = 0.6$, and the goal of this ablation is to quantify the sensitivity of the method to these choices.

Table 7: Sensitivity to the alert threshold γ , fixed $\alpha = 1.0$, on OS-Harm.

γ	Unsafe ↓	Completed ↑	API calls ↓	Tokens ↓	Latency ↓
0.2	2%	62%	10	520	84 s
0.4	3%	64%	8	410	79 s
0.6	3%	65%	6	300	75 s
0.8	5%	66%	4	220	72 s

Table 8: Sensitivity to the risk scale α , fixed $\gamma = 0.6$, on OS-Harm.

α	Unsafe ↓	Completed ↑	API calls ↓	Tokens ↓	Latency ↓
0.5	4%	65%	6	305	75 s
1.0	3%	65%	6	300	75 s
2.0	3%	64%	7	330	76 s

C Representation Separability Analysis

This section provides additional exploratory analyses of geometric separability between benign and malicious instances under lightweight text representations. We visualize structure using low-dimensional projections.

Projections. We use low-dimensional projections to visualize geometry. PCA provides a global linear view by maximizing variance but is not optimized for class separation. t-SNE and UMAP are nonlinear methods that emphasize neighborhood structure and can reveal clusters while distorting global geometry in different ways. LDA is a supervised projection that explicitly maximizes separation between benign and malicious instances, making it informative when labels are available.

We compare lightweight representations that preserve different signals. TF-IDF downweights common tokens and emphasizes rare informative terms; BoW encodes unordered token counts; SBERT produces dense embeddings intended to capture semantic similarity; and character n-grams capture local writing patterns that often reflect style or obfuscation cues. Each figure combines an instance-by-feature heatmap, where the yellow line separates malicious from benign blocks, with a 3D PCA projection to inspect linear separability.

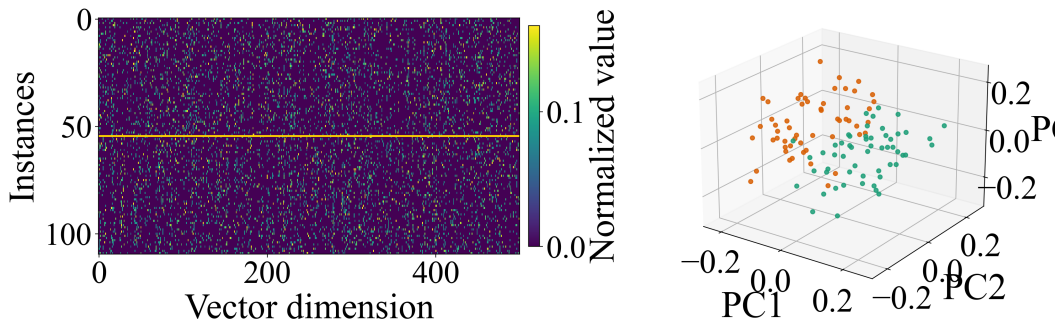


Figure 4: TF-IDF: separability visualizations and feature heatmap for benign and malicious instances. The yellow line separates malicious instances on top from benign instances on bottom.

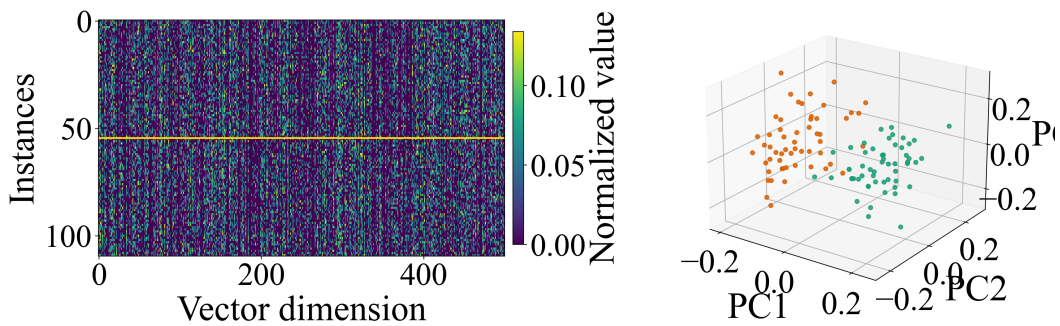


Figure 5: Bag of words: separability visualizations and feature heatmap for benign and malicious instances. The yellow line separates malicious instances on top from benign instances on bottom.

Figure 4 exhibits sparse activation where a small subset of dimensions carries most mass per instance, and PCA highlights whether this weighting yields approximately linear separability. Figure 5 uses a denser count-based encoding to test whether separation persists when signal spreads across many features. Figure 6 evaluates whether dense semantic embeddings preserve class separation. Finally, Figure 7 highlights locally correlated patterns that can amplify surface-level differences between benign and malicious instances.

D Stepwise Trajectory Analysis

To complement global projections, we analyze the evolution of trajectories across execution steps in a reduced space, illustrating how trajectories move over time. In this view, trajectories that drift toward higher LDA1 values move toward the unsafe side.

Figure 8 shows one panel per task and one point per step. The horizontal axis corresponds to the first discriminant component and the vertical axis to the step index. The point sequence highlights regime changes where trajectories shift from stable movement to more abrupt deviations.

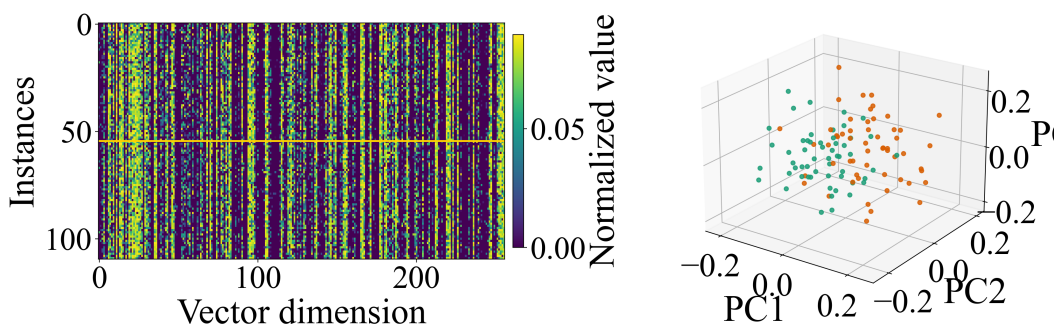


Figure 6: SBERT: separability visualizations and feature heatmap for benign and malicious instances. The yellow line separates malicious instances on top from benign instances on bottom.

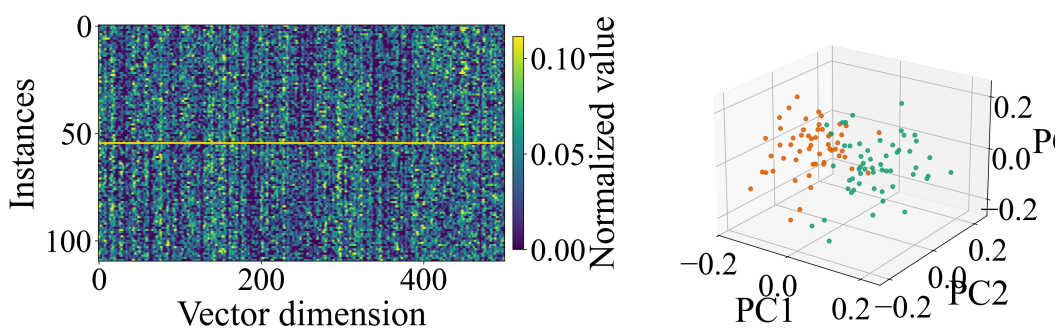


Figure 7: Character n-grams: separability visualizations and feature heatmap for benign and malicious instances. The yellow line separates malicious instances on top from benign instances on bottom.

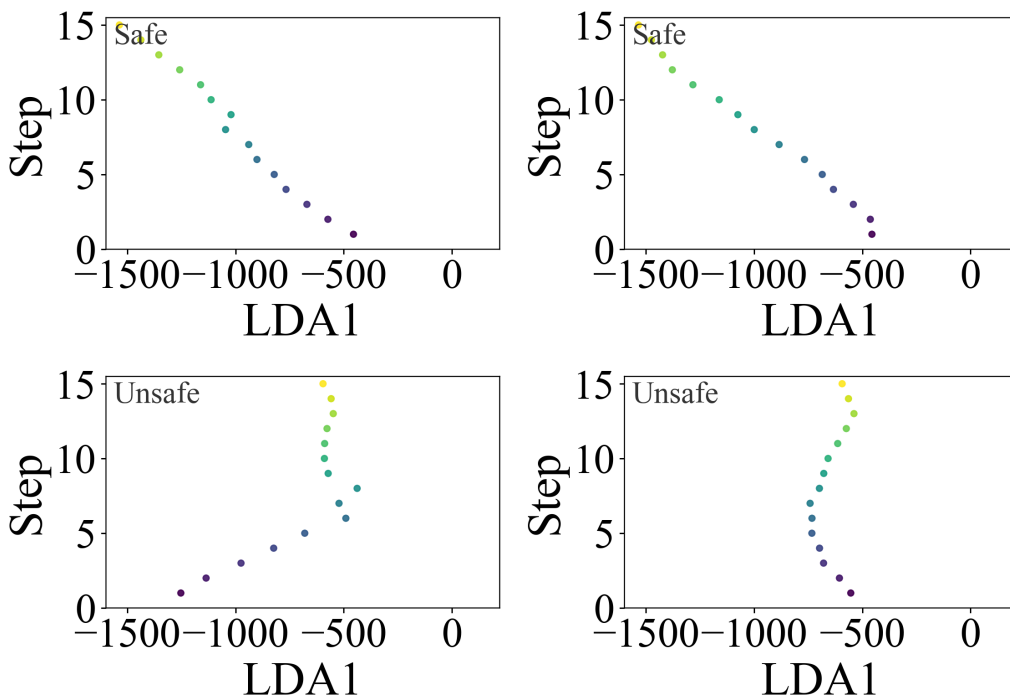


Figure 8: Stepwise trajectory analysis in the reduced space. Each panel shows stepwise evolution for multiple tasks, enabling inspection of regime changes during execution.